Metabolic Engineering 77 (2023) 294–305

Contents lists available at ScienceDirect

Metabolic Engineering

journal homepage: www.elsevier.com/locate/meteng

# Combinatorial gene inactivation of aldehyde dehydrogenases mitigates aldehyde oxidation catalyzed by *E. coli* resting cells

Neil D. Butler, Shelby R. Anderson, Roman M. Dickey, Priyanka Nain, Aditya M. Kunjapur *

*Department of Chemical & Biomolecular Engineering, University of Delaware, Newark, DE, 19716, USA*

ARTICLE INFO

*Keywords:*
Aldehyde
Stability
Oxidation
Biosynthesis
Biocatalysis
Genome engineering
Dehydrogenase

ABSTRACT

Aldehydes are attractive chemical targets both as end products in the flavors and fragrances industry and as synthetic intermediates due to their propensity for C–C bond formation. Here, we identify and address unexpected oxidation of a model collection of aromatic aldehydes, including many that originate from biomass degradation. When diverse aldehydes are supplemented to *E. coli* cells grown under aerobic conditions, as expected they are either reduced by the wild-type MG1655 strain or stabilized by a strain engineered for reduced aromatic aldehyde reduction (the *E. coli* RARE strain). Surprisingly, when these same aldehydes are supplemented to resting cell preparations of either *E. coli* strain, under many conditions we observe substantial oxidation. By performing combinatorial inactivation of six candidate aldehyde dehydrogenase genes in the *E. coli* genome using multiplexed automatable genome engineering (MAGE), we demonstrate that this oxidation can be substantially slowed, with greater than 50% retention of 6 out of 8 aldehydes when assayed 4 h after their addition. Given that our newly engineered strain exhibits reduced oxidation and reduction of aromatic aldehydes, we dubbed it the *E. coli* ROAR strain. We applied the new strain to resting cell biocatalysis for two kinds of reactions – the reduction of 2-furoic acid to furfural and the condensation of 3-hydroxybenzaldehyde and glycine to form a non-standard β-hydroxy-α-amino acid. In each case, we observed substantial improvements in product titer 20 h after reaction initiation (9-fold and 10-fold, respectively). Moving forward, the use of this strain to generate resting cells should allow aldehyde product isolation, further enzymatic conversion, or chemical reactivity under cellular contexts that better accommodate aldehyde toxicity.

## 1. Introduction

Over the last fifteen years, the biosynthesis of aldehydes has risen to prominence across diverse scientific disciplines. The biosynthesis of aldehydes as end products is of high interest in industry, especially as food additives and fragrances (Kunjapur and Prather, 2015). Notable examples of these products have been synthesized in reported literature including the biosynthesis of vanillin from simple carbon sources (Hansen et al., 2009; Kunjapur et al., 2014) or from supplemented precursors (Gallage et al., 2014; Sadler and Wallace, 2021) as well as the biosynthesis of benzaldehyde (Duff and Murray, 1989; Kunjapur et al., 2014, 2016; Orbegozo et al., 2009), piperonal (Schwendenwein et al., 2016), octanal (Horvat and Winkler, 2020), and cinnamaldehyde (Son et al., 2022) from supplemented precursors using microbial cells or enzymes. The last decade has additionally given rise to a plethora of new opportunities for aldehydes to serve as intermediates in biosynthetic pathways or enzyme cascades. Aliphatic aldehydes generated from fermentation or fatty acid synthesis have been used to produce alcohols (Akhtar et al., 2013; Sheppard et al., 2014) or alkanes (Kallio et al., 2014; Sheppard et al., 2016) for applications as fuels and commodity chemicals. Exemplary newer aldehyde-derived biosynthetic targets that have applications in the pharmaceutical and materials industries are tetrahydroisoquinoline alkaloid plant natural products (Pyne et al., 2020), primary or heterocyclic mono-amine precursors to small molecule pharmaceuticals (Citoler et al., 2019; France et al., 2016; Hepworth et al., 2017), diamine polymer building blocks (Fedorchuk et al., 2020; Gopal et al., 2023), hydroxylated non-standard amino acids (Doyon et al., 2022; Ellis et al., 2022; Kumar et al., 2021; Xu et al., 2019, 2020), and β-lactone antibiotics (Schaffer et al., 2017; Scott et al., 2017). Additionally, opportunities to blend biological and abiological synthesis methods to access additional chemical functional groups from aldehydes are emerging, such as the recent chemoenzymatic synthesis of nitriles (Horvat et al., 2022; Winkler et al., 2022).

As these examples illustrate, aldehydes have served as gateways to

* Corresponding author.
*E-mail address:* kunjapur@udel.edu (A.M. Kunjapur).

https://doi.org/10.1016/j.ymben.2023.04.014
Received 13 January 2023; Received in revised form 11 April 2023; Accepted 23 April 2023
Available online 24 April 2023

C–C bond formation and heteroatom introduction due to the electrophilicity of the carbonyl group, enabling diversification of structures and chemical functional groups (Hanefeld et al., 2022; Sulzbach and Kunjapur, 2020). In addition to the biosynthesis of small molecule aldehydes, the biosynthesis of aldehydes on protein residues has been of high academic and commercial relevance since the first application of the formylglycine-generating enzyme on recombinant proteins (Carrico et al., 2007). The post-translational formation of formylglycine residues within proteins introduces an aldehyde tag to enable biologically orthogonal conjugation to small molecules to create conjugate protein therapies. Efforts to improve the cellular environment for aldehyde biosynthesis may offer benefits for protein applications that feature aldehydes.

Despite substantial advances in the ability to biosynthesize aldehydes, two important challenges that limit the ability to feature small molecule aldehydes in cellular environments are their instability due to the activity of cellular enzymes and their toxicity to microbial cells (Dickey et al., 2021). In the last decade, the deletion of some of the many native genes that encode aldehyde reductases in *Escherichia coli* resulted in dramatic improvements in stability for several aromatic and aliphatic aldehydes under aerobic culturing conditions (Kunjapur et al., 2014; Rodriguez and Atsumi, 2014). The deletion of multiple such genes in yeast also contributed to significant improvements in aldehyde stability as observed indirectly through (*S*)-norcoclaurine biosynthesis (Pyne et al., 2020). While at first glance these gene deletion studies appear to have mostly remedied the issue of aldehyde stability for several aldehydes under certain conditions, we sought to test this assumption in more detail. We were particularly curious about aldehyde stability under conditions that could be more relevant for addressing the outstanding issue of aldehyde toxicity. While aldehyde intermediates may be kept at a low steady-state concentration due to the action of downstream enzymes, aldehyde products interfere with cell growth if not immediately separated.

One compelling alternative to the concept of producing aldehyde end products during fermentative growth is to instead harness resting whole cell biocatalysts. The use of such resting cells shares some similarity to the often-employed metabolic engineering strategy of designing a fermentation that features a biomass accumulation phase followed by a production phase. In the case of resting cell biocatalysis, the biological catalyst is first accumulated via a high cell density expression, followed by concentration of the catalyst and resuspension under buffer conditions that enable desired reactions and lack one or more critical macronutrients required for growth (e.g., carbon or nitrogen sources). Resting cell bioconversions offer some advantages over fermentative processes, particularly when a precursor cannot be generated from simple carbon sources, as is the case for several aldehydes of interest, or when the toxicity of a product or intermediate would curtail growth (Lin and Tao, 2017). The use of resting cells can also simplify downstream separations as there are fewer fermentative byproducts. Finally, resting cells also offer some advantages over other alternatives such as cell-free enzyme cascades in that they obviate the need for cell lysis, supplementation of expensive co-factors, or laborious protein purification. Notably, resting cells can still be partially metabolically active, as in many cases glucose is provided to cells for regeneration of co-factors such as ATP and NADPH. Under these cases, they are not growing as they are deprived of nitrogen, sulfur, and other nutrient sources.

In this study, we investigated the stability of biomass-derived aromatic aldehydes when supplemented to either *E. coli* K-12 MG1655 or the engineered RARE (reduced aromatic aldehyde reduction) strain. We examined conditions of aerobic fermentative growth and resting cells prepared after aerobic fermentative growth. We reveal significant differences in the tendency of cells to catalyze aldehyde oxidation under these conditions. In particular, using furfural as a model compound supplemented to engineered strains, we observe that the extent of aldehyde oxidation in resting cells is highly dependent on the growth phase of cell harvesting and the duration of frozen cell storage. Then, we used multiplex automatable genome engineering (MAGE) to perform translational knockouts of several aldehyde dehydrogenases that may contribute to this activity. Engineered strains containing these knockouts achieved significant decreases in the rate of aldehyde oxidation under resting cell conditions, which we then showed can lead to large improvements in aldehyde titer arising from resting cell bioconversions.

## 2. Materials and methods

### 2.1. Strains and plasmids

*Escherichia coli* strains and plasmids used are listed in Table S1. Molecular cloning and vector propagation were performed in DH5α. Polymerase chain reaction (PCR) based DNA replication was performed using KOD XTREME Hot Start Polymerase for plasmid backbones or using KOD Hot Start Polymerase otherwise. Cloning was performed using Gibson Assembly. Oligos for PCR amplification and translational knockouts are shown in Table S2. Oligos were purchased from Integrated DNA Technologies (IDT). The pORTMAGE-EC1 recombineering plasmid was kindly provided by Timothy Wannier and George Church of Harvard Medical School. The DNA sequence and translated sequence of proteins overexpressed can be located in Table S3.

### 2.2. Chemicals

The following compounds were purchased from MilliporeSigma: kanamycin sulfate, dimethyl sulfoxide (DMSO), imidazole, potassium phosphate dibasic, potassium phosphate monobasic, magnesium sulfate, anhydrous magnesium chloride, calcium chloride dihydrate, glycerol, M9 salts, lithium hydroxide, boric acid, Tris base, glycine, HEPES, ATP, 2-napthaldehyde, 4-anisaldehyde, 3-hydroxybenzaldehyde, syringaldehyde, vanillin, benzaldehyde, furfural, 4-hydroxy-3-methoxybenzyl alcohol, furfuryl alcohol, 4-methoxybenzoic acid, 3-hydroxybenzoic acid, syringic acid, vanillic acid, benzoic acid and KOD XTREME Hot Start and KOD Hot Start polymerases. D-glucose, m-toluic acid, piperonal, piperonyl alcohol, 2-naphthol, 4-methoxybenzyl alcohol, 3-hydroxybenzyl alcohol, piperonylic acid, 2-naphthoic acid, and 2-furoic acid were purchased from TCI America. Agarose and ethanol were purchased from Alfa Aesar. Acetonitrile, sodium chloride, LB Broth powder (Lennox), LB Agar powder (Lennox), were purchased from Fisher Chemical. A MOPS EZ rich defined medium kit was purchased from Teknova. Trace Elements A was purchased from Corning. Taq DNA ligase was purchased from GoldBio. Phusion DNA polymerase and T5 exonuclease were purchased from New England BioLabs (NEB). Sybr Safe DNA gel stain was purchased from Invitrogen. Benzyl alcohol was purchased from Merck. 4-hydroxy-3,5-dimethoxybenzoic alcohol was purchased from ChemCruz. NADPH (tetrasodium salt) was purchased from Santa Cruz Biotechnology. Anhydrotetracycline (aTc) was purchased from Cayman Chemical.

### 2.3. Culture conditions

Cultures were grown in LB-Lennox medium (LB: 10 g/L bacto tryptone, 5 g/L sodium chloride, 5 g/L yeast extract), M9 minimal media (Kunjapur et al., 2016) with Corning® Trace Elements A (1.60 μg/mL $CuSO_4 \bullet 5H_2O$, 863.00 μg/mL $ZnSO_4 \bullet 7H_2O$, 17.30 μg/mL Selenite • 2Na, 1155.10 μg/mL ferric citrate) and 1.5% glucose (M9-glucose media), or MOPS EZ rich defined media (Teknova M2105) with 1.5% glucose (MOPS EZ Rich-glucose).

To prepare cells for resting cell assays or cell-free lysate testing for all studies, not including those shown in Fig. 4, confluent overnight cultures of *E. coli* strains were used to inoculate 100 mL cultures in LB media in 500 mL baffled shake flasks. The cultures were grown at 37 °C until mid-exponential phase ($OD_{600}$ = 0.5–0.8), 30 °C for 5 additional hours, and then 18 °C overnight for 18 h. To test the overexpression of different ALDH enzymes in resting cell assays, cultures were grown in LB media

containing antibiotic (50 μg/mL kanamycin) and cultured as described in the prior sentence with 0.2 nM aTc added at mid-exponential phase. For evaluation of resting cell preparation on aldehyde stability, cultures were harvested at mid-exponential phase (grown at 37 °C until a $OD_{600}$ = 0.5–0.8), early stationary phase (grown at 37 °C for 6 h), late stationary phase (18 °C: grown at 37 °C until mid-exponential phase, 30 °C for 5 additional hours, and then 18 °C overnight for 18 h) and late stationary phase (30 °C: grown at 37 °C until mid-exponential phase, 30 °C for 23 h). Cells were then pelleted and frozen at −80 °C.

For growth rate testing, confluent overnight cultures were used to inoculate experimental cultures at 100x dilution in 200 μL volumes in a Greiner clear bottom 96 well plate (Greiner 655090). Cultures were grown for 20 h in a Spectramax i3x plate reader with medium plate shaking at 37 °C. Absorbance readings were taken at 600 nm every 11 min to calculate doubling time and growth rate. For experiments investigating protein expression, strains transformed with a pZE-Ub-sfGFP reporter plasmid were grown as described above with 50 μg/mL kanamycin and 0.2 nM aTc added. In addition, fluorescence readings were taken with excitation at 488 nm and emission at 525 nm every 11 min.

### 2.4. Stability assays

For stability testing under aerobic growth conditions, cultures of each *E. coli* strain to be tested were inoculated from a frozen stock and grown to confluence overnight in 5 mL of LB media. Unless otherwise indicated, confluent overnight cultures were then used to inoculate experimental cultures in 400 μL volumes in a 96-deep-well plate (Thermo Scientific™ 260251) at 100x dilution. Cultures were supplemented with 1 mM of exogenous aldehydes (prepared in 100 mM stocks in DMSO) at mid-exponential phase ($OD_{600}$ = 0.5–0.8). Cultures were incubated at 37 °C with shaking at 1000 RPM and an orbital radius of 3 mm. Samples were taken by pipetting 150 μL from the cultures, centrifuging in a round bottom plate (SPL Life Sciences ISO 13485), and collecting the extracellular broth. Compounds were quantified over a 20 h period using HPLC with samples collected at 4 h and 20 h.

For stability testing under aerobic growth conditions in culture tubes, 5 mL of media were inoculated at 100x dilution with confluent overnights in 14 mL culture tubes. Cultures were supplemented with 1 mM of benzaldehyde (prepared in a 100 mM stock in DMSO) at mid-exponential phase ($OD_{600}$ = 0.5–0.8). Cultures were then incubated at 37 °C in a rotor drum (Thermo Scientific Cel-Gro Tissue Culture Rotator) at maximum speed. Samples were taken via centrifugation after 20 h with compound quantification performed using HPLC.

For resting cell stability testing, cell pellets were thawed (the time period of storage at −80 °C is indicated in each relevant figure caption) and then washed 2x with 200 mM HEPES, pH 7.0 buffer. Masses of cell pellets were measured, and the pellets were resuspended in 200 mM HEPES, pH 7.0 at a wet cell weight of 50 mg/mL, unless otherwise indicated. The resuspended resting cells were then aliquoted into 96-deep-well plates at 400 μL and aldehydes of interest (prepared in 100 mM stocks in DMSO) were added at a concentration of 1 mM. Resting cells were then incubated at 37 °C with shaking at 1000 RPM and an orbital radius of 3 mm. Samples were taken by pipetting 200 μL from the cultures, centrifuging in a round bottom plate, and collecting the extracellular broth. Compounds were quantified over a 20 h period using HPLC with samples collected at 4 h and 20 h.

For lysate stability testing, cell pellets were thawed after being frozen at −80 °C for 7 days and then washed 2x with 5 mL of 200 mM HEPES, pH 7.0 buffer. Cell pellets were then resuspended in 5 mL of 200 mM HEPES, pH 7.0 and disrupted via sonication using a QSonica Q125 sonicator with cycles of 5 s on at 75% amplitude and 10 s off for 5 min. The lysate was distributed into microcentrifuge tubes and centrifuged for 1 h at 18,213×*g* at 4 °C. Supernatant was then collected, and the total protein concentration was then measured using a Bradford assay. Then, the cell-free lysate was concentrated to a final concentration of 5 mg/mL using a 3 kDa cutoff centrifugal concentrator (Amicon Ultra, MilliporeSigma) and aliquoted into 400 μL in 96-deep-well plates and mixed with 1 mM of aldehydes of interest (prepared in 100 mM stocks in DMSO). Cell free lysates were then incubated at 37 °C with shaking at 1000 RPM and an orbital radius of 3 mm. Samples were taken by pipetting 200 μL from the cultures, mixing the sample with 2 μL of 10% trifluoroacetic acid and centrifuging in a round bottom plate, and collecting the extracellular broth. Compounds were quantified after 4 h using HPLC.

### 2.5. Translational genomic knockouts

Translational knockouts to the strain were performed using 10 rounds of MAGE where two stop codons (one TAA and one TGA) were introduced into the genomic sequence for each aldehyde dehydrogenase target in the upstream portion of the gene within the first 30% of amino acids (Table S4). This was performed using the pORTMAGE-EC1 recombineering plasmid (Wannier et al., 2020). Briefly, bacterial cultures were inoculated at 100x dilution from confluent overnight cultures in 3 mL of LB media with 50 μg/mL kanamycin and grown at 37 °C until $OD_{600}$ = 0.5–0.8 was reached. Then, the pORTMAGE plasmid was induced with 1 mM m-toluic acid and cultures were grown at 37 °C for an additional 10 min. Cells were then prepared for electroporation by washing 1 mL three times with refrigerated 10% glycerol and then resuspending in 50 μL of 10% glycerol with each knockout oligo added at 1 μM. Cells were then electroporated and recovered in 3 mL of LB with kanamycin to be used for subsequent rounds. Preliminary assessment of knockouts was performed using PCR and confirmed using Sanger Sequencing. Curing of the pORTMAGE-EC1 plasmid following confirmation of genomic knockouts via serial passaging of the strain produced the ROAR and $ROAR^+$ strains. Whole plasmid sequencing further confirmed the genotype of these strains.

### 2.6. In vitro carboxylic acid reductase activity

For purification, the pZE-niCAR-sfp plasmid was transformed into *E. coli* BL21(DE3). 250 mL of LB in 1 L baffled flasks was supplemented with 50 μg/mL kanamycin and was inoculated at 100x dilution from confluent overnight culture and grown at 37 °C. At mid-exponential phase ($OD_{600}$ = 0.5–0.8), 0.2 nM aTc was added to induce cultures. Cultures were then grown at 30 °C for 5 h and then 18 °C for 18 h. Cells were then harvested by centrifugation.

Next, cells were resuspended in Ni-binding buffer (100 mM HEPES pH 7.4, 250 mM NaCl, 10 mM imidazole, 10% glycerol, 10 mM magnesium chloride). The cells were lysed by sonication followed by centrifugation at 48,000×*g* for 1 h. The cleared supernatant was sterile filtered through a 0.22 μm syringe filter and was purified using AKTA Pure fast protein liquid chromatography (FPLC) system containing a Ni-Sepharose affinity chromatography (HisTrap HP, 5 mL) with isocratic binding, wash and elution steps. Final elution was performed at 250 mM imidazole. Purified fractions were pooled, concentrated, and dialyzed against dialysis buffer (100 mM HEPES pH 7.5, 300 mM sodium chloride, 10% glycerol and 10 mM magnesium chloride hexahydrate) with 30 kDa molecular weight cutoff centrifugal filters (Amicon Ultra, MilliporeSigma).

The *in vitro* CAR assay was performed in a buffer containing 200 mM HEPES, pH 7.0 at 30 °C, 0.5 mM NADPH, 1 mM ATP, 10 mM $MgCl_2$, and 1.5 μM niCAR. To start, 95 μL of the buffer was loaded into a 96 well plate. Prior to spectrophotometric analysis of NADPH depletion, 5 μL of 2-furoic acid (100 mM in DMSO) was added to each reaction well, resulting in final composition of 5 mM 2-furoic acid and 5% v/v DMSO in 100 μL of reaction mix. Oxidation of NADPH was measured at 30 °C for triplicate samples using an Agilent BioTek Synergy H4 Hybrid Microplate Reader at a wavelength of 340 nm for 15 min. Spectral scans of furfural and furoic acid at 5 mM determined that there was no competing absorbance measurement at 340 nm. *In vitro* CAR activity

was then analyzed to determine the maximum rate of NADPH oxidation, using a 0 mM and 0.5 mM NADPH standards as a calibration curve.

### 2.7. Resting cell carboxylic acid reductase screening

To prepare resting cells, the pZE-niCAR-sfp plasmid was transformed into strains of interest. 100 mL cultures in 500 mL baffled shake flasks were supplemented with 50 μg/mL kanamycin and were inoculated at 100x dilution from confluent overnight culture and grown at 37 °C. At mid-exponential phase ($OD_{600}$ = 0.5–0.8), 0.2 nM aTc was added to induce cultures. Cultures were then grown at 30 °C for 5 h and then 18 °C for 18 h. Cells were then harvested by centrifugation and frozen at −80 °C for testing within 2 days.

To assay niCAR in resting cells, we mixed resting cells concentrated to 50 mg/mL wet cell weight in buffer with 200 mM HEPES, pH 7.0, glucose (either 10 or 100 mM concentration for regeneration of ATP and NADPH), 10 mM magnesium chloride, and 5 mM 2-furoic acid in 1 mL volume in 96-deep well plates. Samples were taken by pipetting 200 μL from the cultures, centrifuging in a round bottom plate, and collecting the extracellular broth. Compounds were quantified over a 20 h period using HPLC with samples collected at 1, 2, 4, and 20 h.

### 2.8. Resting cell threonine aldolase screening

To prepare resting cells for threonine aldolase screening, the pZE-EcLTA plasmid was transformed into strains of interest. The over-expression protocol and growth protocol performed was identical to that for cultures containing niCAR.

To assay EcLTA in resting cells, we mixed resting cells concentrated to 50 mg/mL wet cell weight in buffer with 200 mM HEPES, pH 7.0, 100 mM glycine, and 5 mM 3-hydroxybenzaldehyde in 1 mL volume in 96-deep well plates. Samples were taken by pipetting 200 μL from the cultures, centrifuging in a round bottom plate, and collecting the extracellular broth. The relative production of the desired product ((2 S)-2-amino-3-hydroxy-3-(3-hydroxyphenyl)propanoic acid) was quantified over a 20 h period using HPLC with samples collected at 1, 2, 4, and 20 h and product identity confirmed via LC-MS.

### 2.9. HPLC and LC-MS analysis

Metabolites of interest were quantified via high-performance liquid chromatography (HPLC) using an Agilent 1100 Infinity model equipped with a Zorbax Eclipse Plus-C18 column (part number: 959701-902, 5 μm, 95Å, 2.1 x 150 mm). To quantify compounds of interest, an initial mobile phase of solvent A/B = 95/5 was used (solvent A, water, 0.1% trifluoroacetic acid; solvent B, acetonitrile, 0.1% trifluoroacetic acid) and maintained for 5 min. A gradient elution was performed (A/B) with: gradient from 95/5 to 50/50 for 5–12 min, gradient from 50/50 to 0/100 for 12–13 min, gradient from 0/100 to 95/5 for 13–14 min, and equilibration at 95/5 for 14–15 min. A flow rate of 1 mL $min^{-1}$ was maintained, and absorption was monitored at 210, 250, 270, 280 and 300 nm.

To confirm the production of the β-hydroxy non-standard amino acid product produced via threonine aldolase activity, a Waters AQUITY Arc UPLC H-Class with a diode array coupled to a Waters AQUITY QDa Mass Detector was used. The product was analyzed using a Waters Cortecs UPLC C18 column with an initial mobile phase of solvent A/B = 95/5 (solvent A, water, 0.1% formic acid; solvent B, acetonitrile, 0.1% formic acid) and maintained for 5 min. A gradient elution was performed (A/B) with: gradient from 95/5 to 10/90 for 5–7 min, an isocratic flow at 10/90 for 7–10 min, then gradient from 10/90 to 95/5 for 10–10.5 min and a final isocratic step for 10.5–12 min. A flow rate of 1 mL $min^{-1}$ was maintained.

## 3. Results

### 3.1. Aldehydes are subject to unexpected and rapid oxidation under certain incubation conditions with E. coli cells

We first sought to measure the stability of a diverse collection of aromatic aldehydes (Fig. 1A) under aerobic growth conditions in a defined medium (Fig. 1B). In our previous work, we had biosynthesized aldehydes of interest through heterologous expression of the carboxylic acid reductase (CAR) from *Nocardia iowensis* (niCAR) because of the lower toxicity, lower volatility, increased solubility, and possibly superior uptake of carboxylic acid precursors. However, CAR co-expression could mask potential oxidation catalyzed by native cells. To evaluate whether oxidation occurred in fermentative cultures, we supplemented low (1 mM) concentrations of eight different aldehydes to both *E. coli* K-12 MG1655 and the engineered RARE strain in MOPS EZ Rich-glucose media at mid-exponential phase of growth. To screen these eight aldehydes efficiently, we grew cells of either strain in triplicate, 400 μL cultures in deep 96-well plates sealed with non-breathable aluminum seals to limit loss due to aldehyde volatility. We sampled culture broth at two time points (4 h and 20 h after aldehyde addition) to gain some insight on the kinetics of aldehyde stability and to explore whether it could be a function of growth phase. Under these conditions, we observed mostly expected results. In cultures of the wild-type *E. coli* K-12 MG1655 strain, the supplemented aldehydes were nearly completely reduced to their corresponding alcohol within 4 h (Fig. 1C) with this condition persisting after 20 h (Fig. 1D).

In contrast, and as desired, we detected negligible levels of aldehyde reduction and oxidation for these eight aldehydes at 4 h and 20 h after their addition to cultures of the *E. coli* RARE strain (Fig. 1E/F). However, due to the greater volatility of these aldehydes relative to their associated alcohols or acids, we observed greater loss of material when using cells of the RARE strain. This is most noticeable when we supply benzaldehyde (**7**) despite our use of non-breathable seals on the 96-well plates used during both culturing and HPLC sampling. To better examine the case of benzaldehyde addition, we tested growth of RARE cells in capped and sealed 14 mL culture tubes containing 5 mL of media. Under this case, we observed much better preservation of the mass balance, but to our surprise the benzaldehyde had fully oxidized to benzoic acid (Fig. S1). Overall, these experiments indicated that most aldehydes of interest are generally stable in the presence of the RARE strain under aerobic culture conditions, though aldehyde oxidation is possible and a notable concern for benzaldehyde when greater efforts are made to limit its exit from the system.

We next evaluated the stability of these aldehydes when incubated with resting whole cells of either MG1655 or the RARE strain (Fig. 2A). To prepare resting whole cells, we cultured *E. coli* cells aerobically at 37 °C until mid-exponential phase ($OD_{600}$ = 0.5–0.8), 30 °C for 5 additional hours, and then 18 °C overnight for 18 h. We used these growth conditions because they are similar to those used for over-expression of the CAR enzyme, which is often used for aldehyde biosynthesis (Gopal et al., 2023). Following cell culture, we centrifuged the samples and then froze them at −80 °C prior to use for up to one week. To screen stability, we thawed, washed, and resuspended the cells to a working concentration of 50 mg wet cell weight per mL in 200 mM HEPES buffer, pH 7.0. These methods are similar to commonly used whole cell and buffer concentrations for biocatalysis workflows. We then supplied 1 mM aldehyde and monitored stability for 20 h, given biocatalytic whole cell applications are often performed on the time scale of 20–24 h (Horvat et al., 2019), and we additionally took a 4 h time point to investigate stability at time scales pertinent for more active enzymes. By our earliest time point of 4 h after aldehyde addition, we could already observe some aldehyde oxidation using MG1655 cells, which became complete oxidation at our endpoint of 20 h (Fig. 2B–C). For RARE cells, results were nearly equally as surprising, as most aldehydes tested were completely oxidized within 4 h (Fig. 2D–E). To our

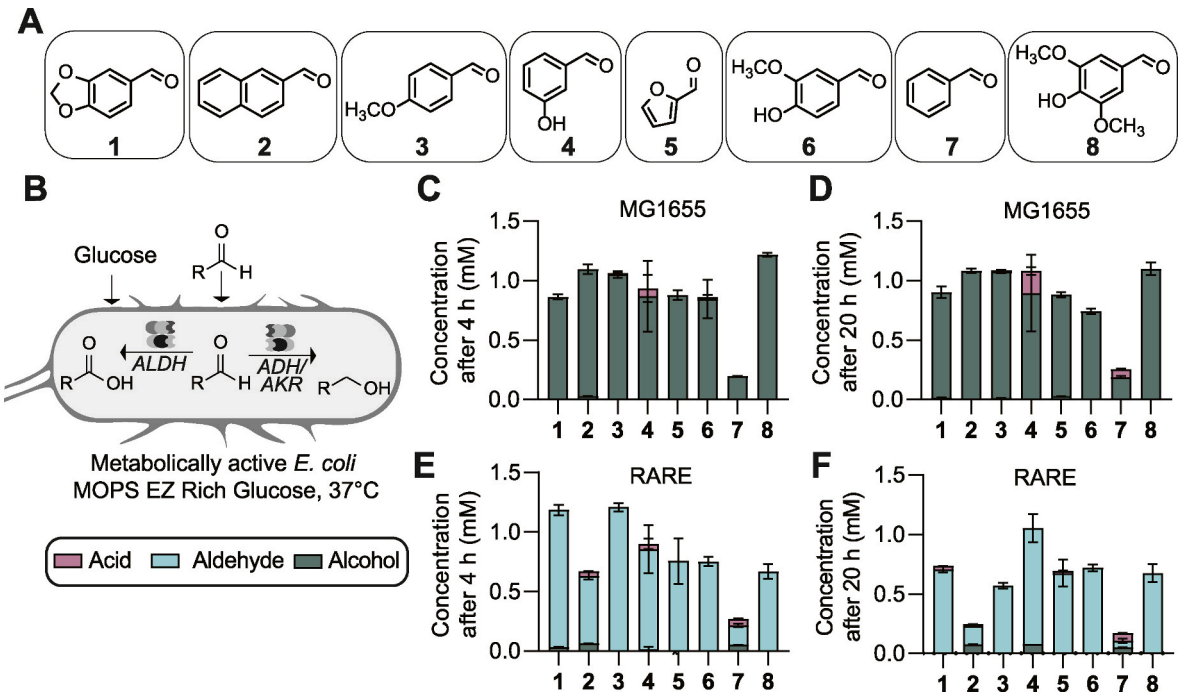


**Fig. 1. Evaluation of the stability of aldehydes when supplemented to aerobic cultures of *E. coli*.** **A.** A panel of lignocellulose-derivable aldehydes was investigated in this study. **B.** Aldehydes were added to culture media to determine when growing *E. coli* cells would catalyze their oxidation or reduction over time. **C.** Cultures of wild-type *E. coli* MG1655 were grown in MOPS EZ Rich-glucose media at 37 °C with supplementation of 1 mM aldehydes, and the fate of the aldehydes in culture media were tracked via HPLC after 4 h. **D.** Measurements from the same cultures taken at 20 h. **E.** Cultures of the previously reported *E. coli* RARE strain (that exhibited reduced aromatic aldehyde reduction for vanillin and benzaldehyde) were grown under identical conditions, and the fate of aldehydes in culture media were tracked via HPLC after 4 h and **F.** 20 h. Data shown is mean of n = 3 with error displayed as standard deviation.

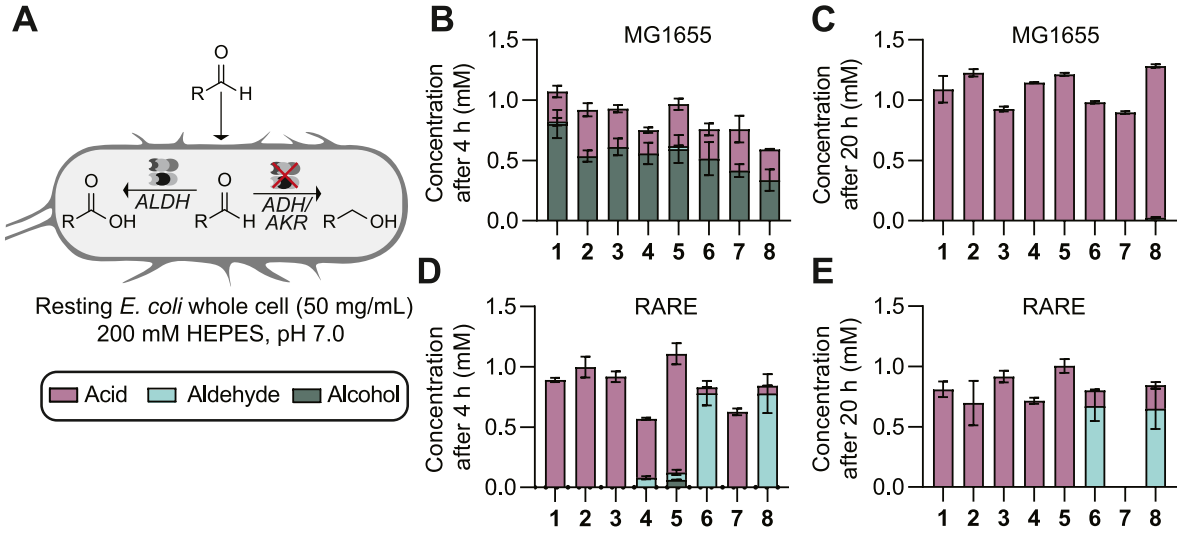


**Fig. 2. Evaluation of the stability of aldehydes in resting whole cell cultures of *E. coli*.** **A.** *E. coli* whole cells were cultured in LB media at 37 °C until mid-exponential phase ($OD_{600}$ = 0.5–0.8), 30 °C for 5 additional hours, and then 18 °C overnight for 18 h. Then, the cells were centrifuged and washed twice in 200 mM HEPES, pH 7.0. Cells were then frozen at −80 °C for 3 (MG1655) or 7 days (RARE) before thawing and resuspension in 200 mM HEPES, pH 7.0 at 50 mg/mL wet cell weight. To initiate experiments, the resuspended whole cells were supplemented with 1 mM aldehydes from our panel (Fig. 1A). **B.** The stability of aldehydes (identity shown in Fig. 1) in resting cells of MG1655 was tracked over 4 h and **C.** 20 h. The stability of aldehydes in resting cells of RARE was tracked over **D.** 4 h and **E.** 20 h. Data shown is mean of n = 3 with error displayed as standard deviation.

knowledge, aldehyde oxidation has never been reported as a phenomenon observed when using resting *E. coli* whole cells. Our data from resting cell experimentation shows that the fate of aldehydes can be substantially altered by deletions of genes encoding oxidoreductase enzymes. It may be governed by factors including the pool sizes of reducing equivalents, a difference in the expression level of oxidoreductases under different conditions, or a difference in the apparent concentrations of these enzymes.

### *3.2. Construction of a new strain by aldehyde dehydrogenase inactivation decreases oxidation*

Given the effectiveness of combinatorial gene deletions at abolishing the reduction of aldehydes and the advancement of multiplexed genome

engineering strategies over the last decade, we next investigated whether we could mitigate the observed oxidation using genome engineering. By performing combinatorial gene inactivation using MAGE, we could discover the potential identity of the genes responsible for oxidation of these aldehydes and discern whether there are major tradeoffs to inactivating these genes (e.g., fitness or protein expression level). To identify aldehyde oxidase enzymes that could be acting upon our aromatic aldehydes of interest, we performed a BLAST search of the *E. coli* K-12 MG1655 genome for the aldehyde dehydrogenase (ALDH) gene *aldB*, which has previously reported oxidative activity upon aromatic aldehydes. From this search, we identified eleven genes exhibiting similarity to *aldB*, with several reported to be active upon aromatic aldehydes (Table 1). We aimed to eliminate the production of AldB and gene products of the five most similar ALDH genes (E-value $<10^{-80}$): *puuC*, *betB*, *patD*, *feaB*, and *gabD*. We used 10 total rounds of MAGE to inactivate each gene in the *E. coli* RARE strain via introduction of in-frame stop codons within the first 30% of codons to obtain a variant that contained all six translational knockouts of these ALDHs (Fig. 3A).

Next, we set out to determine the stability of the set of aromatic aldehydes in resting whole cells of this new strain. Encouragingly, we noticed that aldehyde oxidation after 4 h decreased for all tested aldehydes (Fig. 3B). For a few tested aldehydes, namely piperonal (**1**), 4-anisaldehyde (**3**), 3-hydroxybenzaldehyde (**4**), and furfural (**5**), the difference in stability using the resting cell preparations of the newly engineered strain rather than the RARE strain was quite stark, with retention of over 50% of the supplied aldehyde after 4 h. When having used RARE resting cells, all aldehydes other than vanillin (**6**) and syringaldehyde (**8**) had depleted to less than 10% of their original value, with several aldehydes undetectable. Given these improvements in aldehyde stability, we named our strain the *E. coli* "ROAR" strain for its reduced oxidation and reduction of aromatic aldehydes. Note that in this study we chose to focus on aromatic aldehydes as they are derived from lignocellulose and amenable to facile detection via HPLC-UV; however, it is possible that inactivation of these promiscuous aldehyde dehydrogenases may offer improvements in stabilization of other kinds of aldehydes as well.

### 3.3. Evaluation of additional ALDH knockouts for possible improved aldehyde stability

For applications that feature resting whole cell catalysis, the time frame of 4 h may be sufficient to achieve complete conversion of catalytic processes, but in some cases, longer reaction times may be necessary to achieve desired conversion. At our later time point of 20 h, we observe that resting cells of the ROAR and RARE strains perform comparably poorly at stabilizing tested aldehydes (Fig. 3C). Thus, we then investigated whether additional aldehyde oxidase knockouts could be beneficial for further improving stability. We selected four additional ALDH genes from our original BLAST search having moderately high similarity to that of *aldB* (E-value $<10^{-20}$ in this case): *aldA*, *sad*, *astD*, and *putA* (Table 1). We performed additional cyclic rounds of MAGE to translationally knockout these genes. We then evaluated the stability of our aldehyde set in resting whole cells prepared from this strain ($ROAR^{+}$) rather than the ROAR strain at 4 h (Figs. 3D) and 20 h (Fig. 3E). After 4 h, the $ROAR^{+}$ strain does not appear to provide significantly improved stability over the ROAR strain, with potentially greater oxidation observed in some cases. Similarly, after 20 h, retention of aldehydes is quite poor, with greater instability observed in the case of vanillin (6) and syringaldehyde (8). For three of the aldehydes, piperonal (**1**), *para*-anisaldehyde (**3**), and furfural (**5**), we do appear to observe some retention after 20 h when using cells prepared from the $ROAR^{+}$ strain. However, because the retention is still quite poor (<25% in all three cases) and because of greater oxidation observed after 4 h in some cases, it is unclear if these additional knockouts are beneficial, either due to their substrate scope or expression levels of the ALDHs knocked out (Table 2). Given that we did not discern significant differences in the performance of ROAR and $ROAR^{+}$ in this evaluation, we proceeded ahead with the progenitor ROAR strain instead of the $ROAR^{+}$ strain for further characterization.

**Table 1**
**Native *E. coli* aldehyde dehydrogenase enzymes identified via BLAST search of *aldB*.** All genes shown in bold were investigated for knockout.

| Gene | E-value (*aldB*-basis) | ROAR | ROAR+ | Reported activity on aromatic aldehydes |
|---|---|---|---|---|
| ***aldB*** | 0 | ✓ | ✓ | Benzaldehyde (Ho and Weiner, 2005) |
| ***puuC*** | $5 \times 10^{-109}$ | ✓ | ✓ | Benzaldehyde, Furfural(Jo et al., 2008) |
| ***betB*** | $1 \times 10^{-101}$ | ✓ | ✓ | Benzaldehyde, phenylacetaldehyde ( Falkenberg and Strøm, 1990) |
| ***patD*** | $3 \times 10^{-94}$ | ✓ | ✓ | Benzaldehyde, phenylacetaldehyde, *para*-nitrobenzaldehyde (Gruez et al., 2004) |
| ***feaB*** | $9 \times 10^{-89}$ | ✓ | ✓ | Benzaldehyde, phenylacetaldehyde ( Rodríguez-Zavala et al., 2006) |
| ***gabD*** | $7 \times 10^{-81}$ | ✓ | ✓ | Benzaldehyde, *meta*-nitrobenzaldehyde, *meta*-carboxybenzaldehyde, *para*-carboxybenzaldehyde (Jaeger et al., 2008) |
| ***aldA*** | $3 \times 10^{-79}$ | | ✓ | Benzaldehyde, phenylacetaldehyde ( Rodríguez-Zavala et al., 2006) |
| ***sad*** | $9 \times 10^{-50}$ | | ✓ | |
| ***astD*** | $9 \times 10^{-38}$ | | ✓ | |
| ***putA*** | $3 \times 10^{-37}$ | | ✓ | |
| *maoC* | $2 \times 10^{-16}$ | | | |

### 3.4. Evaluation of aldehyde stability in ROAR fermentations or ROAR cell-free lysate

While aldehydes had been generally stable under aerobic culturing conditions of the RARE strain, we sought to evaluate whether this stability was maintained in the ROAR strain. Here, we found that in 96-well plate aerobic culturing, aldehyde stability was non-distinguishable between the RARE and ROAR strains (Figs. S2A–C). Given that we had previously observed better retention of material and a substantial amount of oxidation when supplying benzaldehyde to cultures grown in culture tubes, we again performed a separate aerobic culturing study in culture tubes (Figs. S2D–E). Here, we saw an improvement in benzaldehyde stability when supplying it to cultures of the ROAR strain, with preservation of about 80% of the aldehyde after 20 h compared to the near complete oxidation that had been observed under these conditions when supplying benzaldehyde to cultures of the RARE strain. This result indicates that ROAR may be a preferred host strain for certain applications of aerobic cultures for metabolic engineering or biocatalysis.

Given the improvement in stability that we observed between aerobic culturing conditions and resting cell conditions, we were also curious about aldehyde stability in concentrated cell-free lysate conditions and whether our gene inactivation might lead to improvements there. When harvesting either RARE or ROAR cells for preparation of concentrated lysates, we observed a very high level of oxidation within 4 h (Fig. S3). This interesting finding indicates that additional genetic modifications may be necessary to inhibit aldehyde oxidation in concentrated lysate, and that, until then, cell-free lysate may not be as attractive a platform as resting cells for aldehyde biosynthesis.

### 3.5. Investigation of the impact of cell harvesting time and cell storage duration on aldehyde stability

Given that the ROAR strain exhibited the largest degree of stabilization under the resting cell conditions, we next sought to probe whether conditions of resting cell preparation could impact aldehyde stability. To start, we evaluated whether the oxidative effect observed in whole cell conditions is impacted by the duration of cell storage at

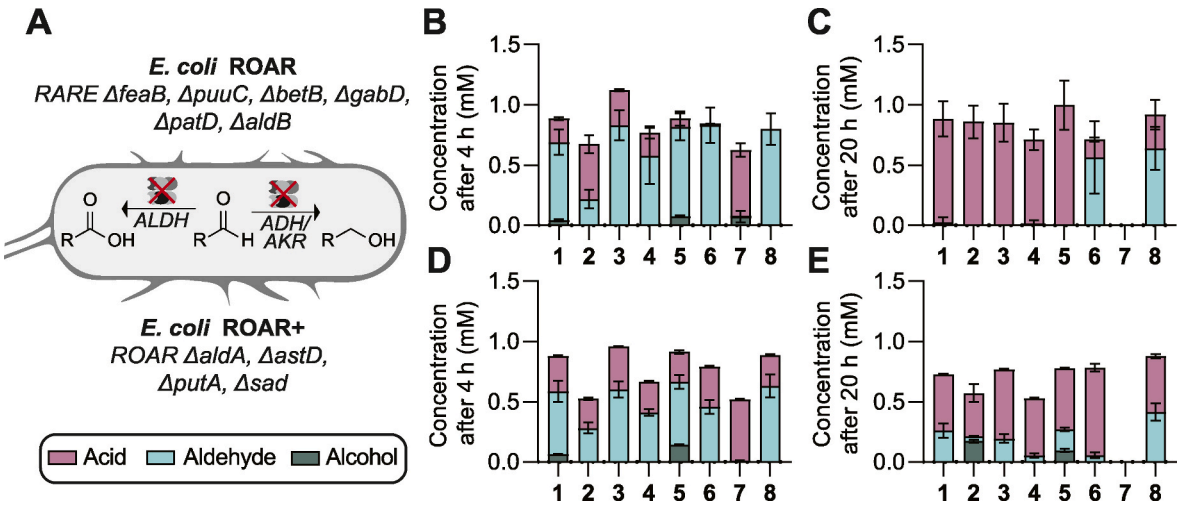


**Fig. 3. Genomic knockout of aldehyde dehydrogenases (ALDHs) toward improved stability in resting whole cell cultures. A.** Using the *E. coli* RARE strain as a basis, multiplexed automatable genome engineering was performed to translationally knockout six ALDHs (*feaB, puuC, betB, gabD, patD, aldB*) to create a strain for reduced oxidation and reduction of aldehydes (ROAR) and a strain with four additional knockouts (*aldA, astD, putA, sad;* ROAR$^{+}$). **B.** *E. coli* ROAR whole cells were cultured in LB media at 37 °C until mid-exponential phase ($OD_{600}$ = 0.5–0.8), 30 °C for 5 additional h, and then 18 °C overnight for 18 h. Then, the cells were centrifuged and washed 2x. Cells were then frozen at −80 °C for 7 days before thawing and resuspension in 200 mM HEPES, pH 7.0 at 50 mg/mL wet cell weight. To initiate experiments, the resuspended cells were supplemented with 1 mM of aldehydes from our panel (Fig. 1A) and the stability of aldehydes in resting cells was tracked over 4 h and **C** 20 h. **D.** *E. coli* ROAR$^{+}$ resting whole cells supplemented with 1 mM aldehydes and the stability of aldehydes in resting cells was tracked over 4 h and **E.** 20 h. Data shown is mean of n = 3 with error displayed as standard deviation.

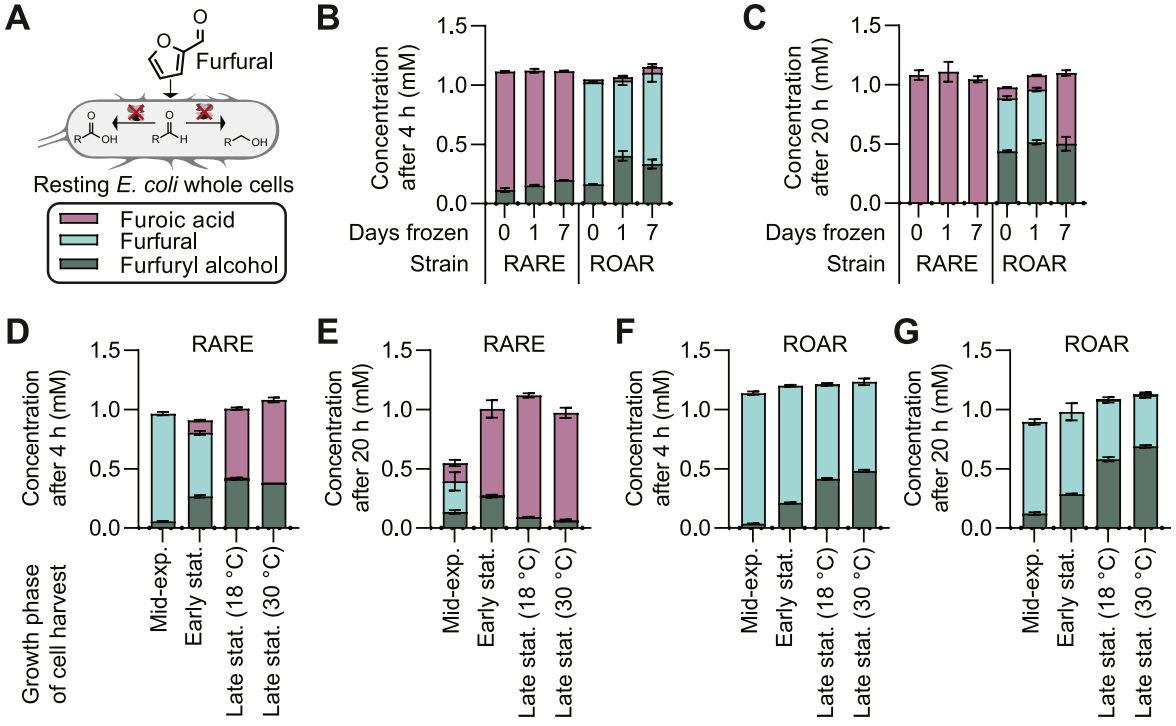


**Fig. 4. Evaluation of resting cell preparation on aldehyde stability. A.** Initial evaluations of stability were performed using furfural as a model aromatic aldehyde supplied at 1 mM concentrations to resting cells of *E. coli* at 50 mg/mL wet cell weight. **B.** Stability of furfural in resting cells of *E. coli* RARE and *E. coli* ROAR was monitored for resting cells that were harvested at late stationary phase and tested fresh (0 days frozen), after 1 day frozen at −80 °C, or after 7 days frozen and monitored after 4 h or **C.** 20 h. **D.** Cells were harvested at various stages of fermentative growth and then stability of furfural was assayed after freezing cells at −80 °C and thawing them the following day. Cell harvest was performed at mid-exponential phase (Mid-exp.; growth at 37 °C for 2 h), early stationary phase (Early stat.; growth at 37 °C for 6 h), and late stationary phase (Late stat.; growth at indicated temperature for 18 h) for evaluation of furfural stability after 4 h and **E.** 20 h in RARE and **F.** in ROAR at both 4 h and **G.** 20 h. Data shown is mean of n = 3 with error displayed as standard deviation.

−80 °C following harvest or by the freezing and thawing of cells. We performed resting whole cell stability testing using RARE and ROAR strains (Fig. 4A–C), where harvested cells were either assayed fresh (0 days), frozen for 24 h (1 day), or frozen for 7 days. We supplied furfural to resting cells in these experiments, as it had been well stabilized at the 4 h timepoint in earlier experiments. The results indicate that one instance of freeze-thaw of cells does not impact the stability of aldehydes upon supplementation to resting cells. However, after 7 days of storage,

**Table 2**
Percent of aromatic aldehyde in resting whole cell conditions after 4 h.

| Aldehyde | RARE (%) | ROAR (%) | ROAR$^+$ (%) |
|---|---|---|---|
| 1 | 0 | 65 ± 11 | 52 ± 9 |
| 2 | 0 | 22 ± 8 | 28 ± 5 |
| 3 | 0 | 83 ± 12 | 60 ± 7 |
| 4 | 8 ± 1 | 58 ± 23 | 41 ± 3 |
| 5 | 6 ± 2 | 77 ± 7 | 50 ± 8 |
| 6 | 78 ± 10 | 83 ± 15 | 46 ± 6 |
| 7 | 0 | 0.50 ± 0.05 | 1.1 ± 0.2 |
| 8 | 78 ± 16 | 80 ± 13 | 63 ± 9 |

rather than 0 or 1 day of storage, resting whole cells of ROAR exhibit greater oxidation of furfural 20 h after its addition. The appearance of oxidation more closely resembles what had previously been observed from cells tested 7 days post-harvest (Fig. 3) and suggested that the oxidative driving force may increase with storage time in resting ROAR cells. We also saw greater levels of furfural reduction during these experiments regardless of the duration of storage.

Having observed the influence of storage duration, we next sought to understand whether the duration of culturing prior to harvesting cells could affect furfural stability observed in resting cell experiments. In this case, cells were frozen for only 24 h prior to assaying stability (Fig. 4D–G). Here, we found that in the RARE strain, the later that cells were harvested, the more rapidly furfural oxidation appeared to occur. In contrast, for the ROAR strain, the later that cells were harvested, the greater the degree of furfural reduction we observed. Cells should contain less reducing power as time passes after depletion of a growth-limiting carbon source; while it is tempting to speculate that cells would therefore be more likely to catalyze aldehyde oxidation when harvested at later times, our observations using the ROAR strain are in conflict with that. Instead, our data suggests that the presence or absence of certain native aldehyde dehydrogenases contributes to differences in the fate of supplemented aldehydes under otherwise identical growth, storage, and assay conditions. To investigate this further, we assessed the stability of the aromatic aldehyde panel in ROAR and ROAR$^+$ resting cells harvested at early stationary phase and resuspended within 24 h of harvest (Fig. S4). For the ROAR strain, the effect of cell harvesting time on the stability of most of the aldehydes is not particularly pronounced, though we do see greater reduction under these cases for several other aldehydes. Stability in ROAR$^+$ under these conditions was fairly improved, as only modest (less than 50%) oxidation was measured across the aldehyde panel, and aldehyde retention at 4 h was quite high. However, after 20 h, several aldehydes (**1**, **2**, **3**, **4**, and **5**) exhibit reduction. For applications in aldehyde biocatalysis, considerations should be made to balance the timing of cell harvest with the timing which maximizes the titer of the enzymatic catalyst. For enzymes which require large outgrowth for maximum titer and reaction incubation for greater than 4 h, the ROAR strain will likely be preferable.

### 3.6. Screening of ALDH activity on an aldehyde of interest

In this study, a total of 10 ALDH knockouts were performed, all bearing homology to ALDH's with reported activity on aromatic aldehydes. Given this similarity, we believed that most of these enzymes are likely to be active upon the aldehydes screened. To test this hypothesis, we cloned the ALDHs into plasmid-based vectors and overexpressed them in the ROAR$^+$ strain. Using resting cells harvested at late stationary phase and frozen for 24 h, we evaluated the stability of furfural in this case compared to resting cells of RARE, ROAR, and ROAR$^+$. Resting cell stability screening indicates that all these genes except for *patD* and *putA* have some oxidative activity on furfural (Fig. S5). Given the ROAR and ROAR$^+$ strains do not exhibit significant differences in furfural stability, this result is somewhat unexpected and indicates that the basal expression levels of some the ALDHs knocked out in the ROAR$^+$ strain may be low.

### 3.7. Characterization of the ROAR strain for biocatalysis applications

In addition to the metric of aldehyde stabilization, a host strain used for whole cell biocatalysis must exhibit a robust growth rate and an ability to overproduce catalytic proteins of interest. Thus, we next investigated whether the ROAR or ROAR$^+$ strains could achieve comparable growth rates and protein titers as the RARE strain or its progenitor, the wild-type MG1655 strain. Encouragingly, in complex media such as LB, which is commonly used for protein overexpression, we do not see significant differences in the growth curve or doubling time between the wild-type MG1655 or engineered strains (Fig. 5A), with average doubling times of 22–28 min at 37 °C. In defined media such as M9-glucose minimal media or MOPS EZ Rich-glucose, which can also be optimal for maximal control of media conditions or for growth in industrial scale bioreactors, ROAR appears to grow marginally slower with a doubling time of ~62 min compared to ~46 min in MG1655 in M9-glucose and ~27 min compared to ~23 min in MOPS EZ Rich-glucose, but ROAR$^+$ does not appear to exhibit significantly different growth than MG1655 (Fig. 5B, Fig. S6A). Next, we investigated the level of production of a superfolder green fluorescent protein (sfGFP) reporter from a plasmid expression vector transformed separately into each of the three strains. We observe comparable $OD_{600}$-normalized production of sfGFP in LB, M9-glucose, and MOPS EZ-glucose media across all strains tested (Fig. 5C–D, Fig. S6B). In general, and in resting cell complementary media conditions, ROAR and ROAR$^+$ grow and produce protein at levels likely sufficient for biocatalysis compared to MG1655 (doubling times are within 35% for all media tested).

For some whole cell applications, such as biocatalytic conversions of acids to aldehydes using the CAR enzyme, whole cells are not supplied with a nitrogen source but are supplied with glucose to enable cofactor recycling through glycolysis. With this in mind, we next interrogated whether the presence of carbon sources may impact stability in the whole cell condition. Here, we found that when concentrated whole cells were supplied with glucose and furfural, substantial furfural reduction occurred when using either RARE or ROAR (Fig. S7). Previous studies have demonstrated that in the presence of a carbon feedstock under conditions of nitrogen starvation (Brauer et al., 2006), *E. coli* accumulates higher concentrations of both NADH and NADPH. This suggests that under additional reductive power an increase in furfural reduction can occur regardless of the deletions of oxidoreductase genes in these strains.

### 3.8. Application of the ROAR strain in aldehyde biocatalysis

It is anticipated that resting cell preparations of the ROAR strain could be useful for diverse aldehyde biosynthetic processes, and to shed some light on this, we examined the biosynthesis of furfural (**5**) from its associated carboxylic acid, 2-furoic acid. These are both versatile platform compounds derived from lignocellulosic biomass, though furfural strongly inhibits bacterial growth. Here, we aimed to use niCAR, an NADPH and ATP-dependent enzyme from *N. iowensis* to perform this bioconversion as this enzyme has been demonstrated to exhibit broad substrate specificity. To start, we investigated whether niCAR was active upon furoic acid by using an *in vitro* assay. We tracked activity via consumption of NADPH (quantified via measurement of absorbance at 340 nm). Our experiment indicated that niCAR was active on the substrate of interest (Fig. S8). With this result, we then proceeded to prepare resting whole cells of both the RARE strain and the ROAR strain after transformation with an appropriate plasmid that co-expresses niCAR and the phosphopantetheinyl transferase *Sfp* from *Bacillus subtilis* which is required for CAR activation. In this case, we omitted the ROAR$^+$ strain since it did not appear to further stabilize furfural. We used culturing conditions that maximized niCAR production during fermentation. We cultured *E. coli* cells aerobically at 37 °C until mid-exponential phase ($OD_{600}$ = 0.5–0.8) at which point niCAR synthesis was induced. Then, cultures were further incubated at 30 °C for an additional 5 h, 18 °C

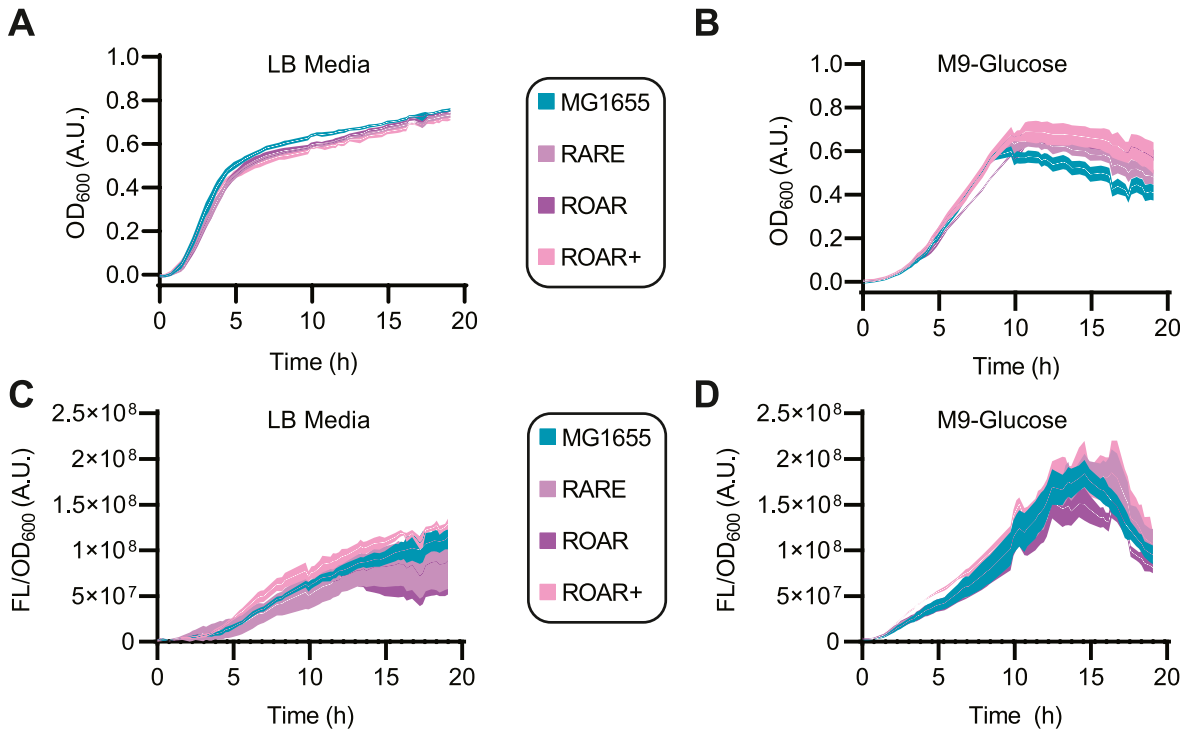


**Fig. 5. Growth and protein production performance of engineered aldehyde retaining strains. A.** Growth was monitored via optical density at 600 nm ($OD_{600}$) measured in 96-well plate 20 h in LB media and **B.** in M9-glucose minimal media. **C.** Plasmid-based protein overexpression of superfolder green fluorescent protein (sfGFP) was monitored via 96 well plate in a plate reader for 20 h by measuring fluorescence (ex: 488 nm, em: 525 nm) normalized by $OD_{600}$ in both LB media and **D.** M9-glucose minimal media. The abbreviation A.U. indicates arbitrary units. Data shown is mean of n = 3 with error displayed as standard deviation with the curve smoothed between data points taken approximately every 10–20 min.

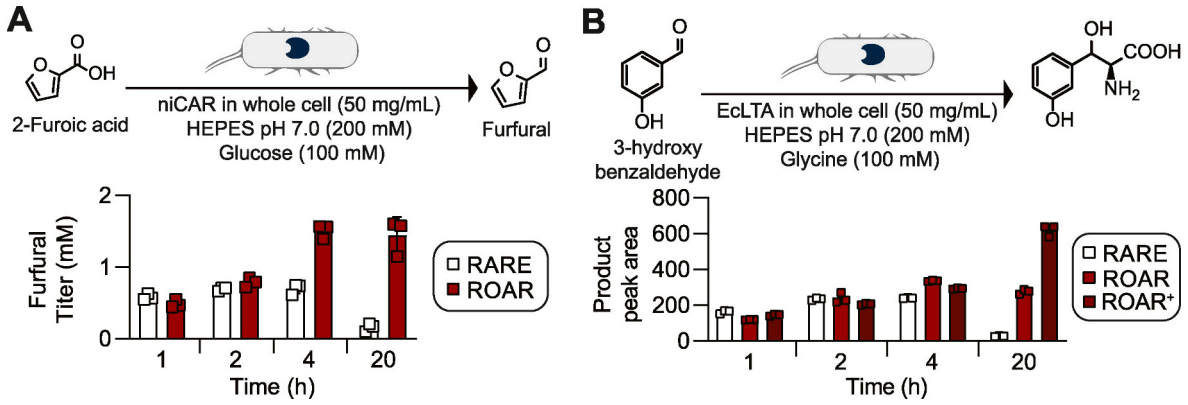


**Fig. 6. Applications of ROAR in resting whole cell catalysis. A.** The carboxylic acid reductase from *Nocardia iowensis* (niCAR) can reduce aromatic carboxylic acid at the cost of one NADPH and one ATP to form aldehydes. To synthesize furfural, resting whole cell biocatalysts of RARE or ROAR (50 mg/mL wet cell weight) containing overexpressed niCAR were incubated at 30 °C with 100 mM glucose for cofactor regeneration and 5 mM 2-furoic acid to measure conversion between the two strains. **B.** Threonine aldolase from *E. coli* synthesizes beta-hydroxy amino acids in the presence of excess glycine. Resting whole cells of RARE, ROAR, and $ROAR^{+}$ containing overexpressed EcLTA (50 mg/mL) were incubated at 30 °C with 100 mM glycine to drive the reaction forward. Product was measured via peak area. Data shown are each individual replicate (n = 3) with mean displayed and error displayed as standard deviation.

overnight for 18 h, and then harvested by centrifugation. After harvesting of cells, these were frozen for 24 h before resuspension in HEPES buffer. To perform the reaction, these resting cells were mixed with 5 mM of 2-furoic acid substrate and glucose at concentrations of either 10 mM or 100 mM. Glucose is provided to regenerate the cofactors needed by niCAR (Fig. 6A, Fig. S9). We proceeded to monitor production of furfural over time, where we were excited to see that by 4 h the ROAR strain outperformed the RARE strain by over 2-fold in measured furfural titer when using 100 mM glucose (0.70 ± 0.07 mM using RARE, 1.51 ± 0.10 mM using ROAR) or 10 mM glucose (0.78 ± 0.09 mM using RARE, 1.87 ± 0.04 mM using ROAR). When monitoring the reaction for 20 h, we were excited further still to observe that the ROAR strain was able to maintain its production of furfural (1.45 ± 0.26 mM) while reactions in the RARE strain resulted in significant loss of product (0.16 ± 0.06 mM). Thus, use of the ROAR strain achieved a nearly 9-fold enhancement in final furfural titer when using 100 mM glucose. We saw similar average results when providing 10 mM glucose but with greater standard deviation at the 20 h time point.

We then sought to investigate whether the stabilization provided by the ROAR strain could improve biocatalysis using an application wherein an aldehyde is a reagent. To do so, we looked into the enzyme class L-threonine aldolase (LTA), which natively catalyzes the reversible

cleavage of L-threonine or non-natural L-β-hydroxy-α-amino acids to form glycine and the corresponding aldehydes (Fesko, 2016, 2019). In biocatalysis, LTAs are of particular interest for the reverse reaction where they catalyze formation of β-hydroxy-α-amino acids when supplemented with excess glycine and an aldehyde. Here, we evaluated the capability of the ROAR and ROAR$^+$ strains to improve the conversion of 3-hydroxybenzaldehyde to the corresponding L-β-hydroxy-α-amino acid as compared to the RARE strain. Using resting cells that overexpressed *E. coli* LTA (EcLTA), we observed that the transformed ROAR and ROAR$^+$ strains achieve mildly higher product peak areas compared to the RARE strain after 4 h (Fig. 6B, Figs. S9–11). However, after 20 h, we see substantial improvement in titers achieved using the ROAR and ROAR$^+$ strains compared to the RARE strain with ~10-fold enhancement in the ROAR strain case and ~22-fold enhancement in the ROAR$^+$ strain case. Thus, we have shown that the genetic engineering performed to create the ROAR strain leads to substantial improvements in the stabilization of aldehydes during resting cell conditions and that this improved stabilization can be beneficial during bioconversions that form aldehydes.

## 4. Discussion

In this work, we identified that an *E. coli* strain engineered for aldehyde stabilization, the RARE strain, is effective at stabilizing diverse biomass-derived aromatic aldehydes under aerobic growth conditions but does not stabilize aldehydes under resting whole cell conditions. Recently, many researchers have taken to characterizing the activity of aldehyde-associated enzymes, either producers or consumers, in the resting whole cell condition (Doyon et al., 2022; Hepworth et al., 2017). Resting whole cell biocatalysts offer several practical advantages compared to alternatives of fermentation and purified protein biocatalysis, such as simple catalyst separation, no need for cell lysis nor enzyme purification steps, and the ability to tolerate conditions (compounds, solvents, and pH/temperature) that inhibit growth. Our work indicates that previous applications of the RARE strain had not identified aldehyde oxidation because of important differences between aerobic culturing and resting cell conditions, even though our resting cells had been cultured aerobically prior to harvesting. Additionally, unlike in many previous studies, here we did not evaluate aldehyde stability with heterologous expression of highly active CAR enzymes, whose reductive activity can mask the oxidative effects we observed here. For many preferred substrates of CAR enzymes, CAR expression could serve to eliminate perceived oxidation, but this would occur in competition with native aldehyde dehydrogenase activity, leading to futile consumption of ATP and NADPH. An engineering solution to eliminate aldehyde oxidation, as opposed to counteracting it, can avoid this futile cycle.

Here, we used the combinatorial genome engineering technique of MAGE to rapidly terminate the synthesis of full-length ALDHs. Natively, ALDH genes serve several purposes in catabolism and cellular function more broadly with applications in lysine catabolism (glutarate semialdehyde dehydrogenase, *gabD*) (Knorr et al., 2018), phenylalanine degradation (phenylacetaldehyde dehydrogenase, *feaB*) (Rodríguez-Zavala et al., 2006), osmolyte synthesis (betaine aldehyde dehydrogenase, *betB*) (Falkenberg and Strøm, 1990), and general toxification of aldehydes (*aldB*) (Ho and Weiner, 2005). Many ALDHs were previously reported to be fairly promiscuous, with activity identified across ranges of both aliphatic substrates and aromatic substrates. For example, AldB is reported to act on aldehydes as distinct as benzaldehyde and acetaldehyde. Given the broad literature-evidenced polyspecificity of these enzymes, we used the speed and ease of MAGE to target different groups of genes, investigating ten different ALDH targets in two different pools of knockouts.

We found that translational knockout of an initial pool of six highly similar ALDHs with reported activity on aromatic aldehydes was sufficient to improve the retention of several aromatic aldehydes as compared to RARE after 4 h. We termed our newly engineered strain that contained the inactivation of all six initial candidate ALDH genes (Δ*aldB*, Δ*puuC*, Δ*betB*, Δ*patD*, Δ*feaB*, and Δ*gabD*) the *E. coli* ROAR strain. We then investigated the knockout of four additional ALDH genes using MAGE, though the improvement in stability afforded by these mutations was minimal. When evaluating variants of this more engineered strain (ROAR$^+$) with ALDHs overexpressed, we found that eight of the ten ALDHs (the exceptions being PatD and PutA) appear to be active on furfural, indicating that the redundancy in aromatic aldehyde oxidative activity is quite high. The degree of stabilization, however, is somewhat dependent on the timing of cell harvest. Here, we found that freshly harvested cells and those harvested in earlier stages of cell growth exhibit greater stability than those stored for a week or harvested at late stationary phase. These aspects will be important to consider when utilizing the ROAR strain for biocatalysis. Although we did not completely abrogate the phenomenon of aldehyde oxidation in most cases, which remains dominant at longer (20 h) time scales, we succeeded in demonstrating substantial improvements in aldehyde stability at shorter (4 h) time scales. These time scales should be more relevant for resting cell biocatalysis processes, especially those that involve aldehyde separation, aldehyde consumption by desired downstream enzymes, or catalyst separation through systems such as flow reactors.

In our previous work to limit the native reduction of aldehydes in metabolically active cells, culminating in the creation of the RARE strain, we knocked out six different aldehyde reducing genes from two distinct families of enzymes, the NADPH-dependent aldo-keto reductase (AKR) family and the NADH-dependent alcohol dehydrogenase (ADH) family (Kunjapur et al., 2014). Reduction was significantly decreased for the model aldehydes tested in that work (benzaldehyde and vanillin) and for other aromatic and aliphatic aldehydes tested in follow-on work. Here, we further characterized the RARE strain and noted the stabilization for all eight of the target aromatic aldehydes under aerobic growth conditions. Similarly, in the creation of ROAR, we targeted six genes for knockout which were sufficient to achieve noted improvement in stability, this time limiting oxidation in the resting cell condition. Conversely, in this study, we only targeted gene products from a single family, the NADH-dependent ALDH family of enzymes. Another aldehyde oxidizing enzyme from a different family has been reported in *E. coli* previously, namely the periplasmic, molybdenum-dependent aldehyde oxidase PaoABC, with specificity for aromatic aldehydes (Correia et al., 2016; Neumann et al., 2009). As this enzyme appears to have strict dependence for acidic conditions (pH $< 6$) in order to exhibit activity, it was not investigated in this work. After creating the ROAR strain, we characterized it for attributes other than aldehyde stabilization and noticed little to no effect on growth or heterologous protein expression, depending on the medium used. As in the case of the RARE strain, this is fortuitous because ALDHs are a highly redundant enzyme class within *E. coli* and are believed to serve important roles in several catabolic pathways. Together, these studies reveal that multiple groups of redundant oxidoreductase enzymes (ADHs, AKRs, and ALDHs) can all be swiftly removed from bacterial cells using combinatorial genome engineering approaches, and that these enzymes are not critical to the cell under a wide range of laboratory conditions. However, unlike in the case of RARE, which afforded nearly complete elimination of aldehyde reduction even at long timescales, the improvements seen in this study are eventually overcome by remaining activity of native enzymes.

Several biosynthetic pathways involving aldehydes as substrates, intermediates, or products can benefit from the improved stability of aromatic aldehydes. Numerous industrially important PLP-dependent enzyme classes including threonine aldolases, threonine transaldolases, and transaminases all utilize aldehydes as substrates for biocatalysis (Doyon et al., 2022; Slabu et al., 2017; Song et al., 2018). Several recent efforts have looked to profile these enzymes in whole cell biocatalysts for ease of catalyst recovery relative to cell-free enzymatic reactions, ease of product separation relative to fermentative contexts, higher throughput screening using cell-based assays on shorter

timescales, and greater consistency of production relative to fermentative contexts. In addition, the cost of whole cell catalysts is far lower than purified enzymes and this difference increases as enzyme cascades became longer and require more ancillary enzymes for co-factor or catalyst regeneration.

Here, we demonstrated that the ROAR strain can offer notable improvements for biocatalysis with examples including an aldehyde as a product and a reagent. First, we catalyzed the production of the aldehyde furfural via reduction from 2-furoic acid via resting cells expressing a carboxylic acid reductase. We observed improvements in aldehyde product retention even at long time scales when paired with CAR expression. The reduction of 2-furoic acid to furfural resulted in a 2-fold enhancement in furfural titers when using resting cells of the ROAR strain rather than the RARE strain 4 h after reaction initiation and a nearly 9-fold enhancement in furfural titers 20 h after reaction initiation. For an aldehyde end product, extractive protocols can and should be used to help limit loss due to volatility or oxidation and toxicity. However, utilization of a strain with diminished oxidation can provide complementary and dramatic improvements to performance, and we expect this to be more consequential at the higher substrate loadings that would be of greater industrial relevance. For applications of resting cells where an aldehyde is a reagent, we assessed whether the ROAR strains could improve resting cell biocatalytic applications for the LTA enzyme. Here, we found improvement in the condensation of 3-hydroxybenzaldehyde with glycine to form a beta-hydroxylated amino acid product, achieving ~10-fold enhancement in beta-hydroxy amino acid production in the ROAR strain and ~22-fold enhancement in the ROAR$^{+}$ strain. Our future work will look to identify whether inefficiencies in resting cell biocatalysts that feature other enzyme classes could be overcome using the ROAR strain.

## Author statement

A.M.K. conceived and supervised the study, performed experiments that first created and prototyped the ROAR strain, and helped write the manuscript; N.D.B. designed and conducted all stability experiments, analyzed data, prepared figures, and wrote most of the manuscript; S.R.A. performed the MAGE to create ROAR and performed growth and protein production assays in addition to experiments in Fig. 6B; R.M.D. performed the MAGE to create ROAR$^{+}$, experiments in Fig. 4D–G, Fig. S5, and Fig. S7; P.N. initially documented and characterized the phenomenon of aldehyde oxidation in our lab and prepared strains for niCAR testing and performed experiments in Fig. 4A–C.

## Declaration of competing interest

None.

## Data availability

Data will be made available on request.

## Acknowledgements

We acknowledge support from the following funding sources: The National Science Foundation (NSF CMMI-1934887 and CBET-2032243) and minor support from the Center for Plastics Innovation, an Energy Frontier Research Center funded by the U.S. Department of Energy (DOE), Office of Science, Basic Energy Sciences, under Award No. # DE-SC0021166.

## Appendix A. Supplementary data

Supplementary data to this article can be found online at https://doi.org/10.1016/j.ymben.2023.04.014.

## References

Akhtar, M.K., Turner, N.J., Jones, P.R., 2013. Carboxylic acid reductase is a versatile enzyme for the conversion of fatty acids into fuels and chemical commodities. Proc. Natl. Acad. Sci. USA 110, 87–92. https://doi.org/10.1073/pnas.1216516110.

Brauer, M.J., Yuan, J., Bennett, B.D., Lu, W., Kimball, E., Botstein, D., Rabinowitz, J.D., 2006. Conservation of the metabolomic response to starvation across two divergent microbes. Proc. Natl. Acad. Sci. USA 103, 19302–19307. https://doi.org/10.1073/pnas.0609508103.

Carrico, I.S., Carlson, B.L., Bertozzi, C.R., 2007. Introducing genetically encoded aldehydes into proteins. Nat. Chem. Biol. 3, 321–322. https://doi.org/10.1038/nchembio878.

Citoler, J., Derrington, S.R., Galman, J.L., Bevinakatti, H., Turner, N.J., 2019. A biocatalytic cascade for the conversion of fatty acids to fatty amines. Green Chem. 21, 4932–4935. https://doi.org/10.1039/C9GC02260K.

Correia, M.A.S., Otrelo-Cardoso, A.R., Schwuchow, V., Sigfridsson Clauss, K.G.v., Haumann, M., Romão, M.J., Leimkühler, S., Santos-Silva, T., 2016. The *Escherichia coli* periplasmic aldehyde oxidoreductase is an exceptional member of the xanthine oxidase family of molybdoenzymes. ACS Chem. Biol. 11, 2923–2935. https://doi.org/10.1021/acschembio.6b00572.

Dickey, R.M., Forti, A.M., Kunjapur, A.M., 2021. Advances in engineering microbial biosynthesis of aromatic compounds and related compounds. Bioresour. Bioprocess 8, 91. https://doi.org/10.1186/S40643-021-00434-X.

Doyon, T.J., Kumar, P., Thein, S., Kim, M., Stitgen, A., Grieger, A.M., Madigan, C., Willoughby, P.H., Buller, A.R., 2022. Scalable and selective β-Hydroxy-α-Amino acid synthesis catalyzed by promiscuous <scp>l</scp> -threonine transaldolase ObiH. Chembiochem 23, e202100577. https://doi.org/10.1002/cbic.202100577.

Duff, S.J.B., Murray, W.D., 1989. Oxidation of benzyl alcohol by whole cells of *Pichia pastoris* and by alcohol oxidase in aqueous and nonaqueous reaction media. Biotechnol. Bioeng. 34, 153–159. https://doi.org/10.1002/bit.260340203.

Ellis, J.M., Campbell, M.E., Kumar, P., Geunes, E.P., Bingman, C.A., Buller, A.R., 2022. Biocatalytic synthesis of non-standard amino acids by a decarboxylative aldol reaction. Nat. Catal. 5, 136–143. https://doi.org/10.1038/s41929-022-00743-0.

Falkenberg, P., Strøm, A.R., 1990. Purification and characterization of osmoregulatory betaine aldehyde dehydrogenase of *Escherichia coli*. Biochim. Biophys. Acta Gen. Subj. 1034, 253–259. https://doi.org/10.1016/0304-4165(90)90046-Y.

Fedorchuk, T.P., Khusnutdinova, A.N., Evdokimova, E., Flick, R., di Leo, R., Stogios, P., Savchenko, A., Yakunin, A.F., 2020. One-Pot biocatalytic transformation of adipic acid to 6-aminocaproic acid and 1,6-hexamethylenediamine using carboxylic acid reductases and transaminases. J. Am. Chem. Soc. 142, 1038–1048. https://doi.org/10.1021/jacs.9b11761.

Fesko, K., 2019. Comparison of L-threonine aldolase variants in the aldol and retro-aldol reactions. Front. Bioeng. Biotechnol. 7.

Fesko, K., 2016. Threonine aldolases: perspectives in engineering and screening the enzymes with enhanced substrate and stereo specificities. Appl. Microbiol. Biotechnol. 100, 2579–2590. https://doi.org/10.1007/s00253-015-7218-5.

France, S.P., Hussain, S., Hill, A.M., Hepworth, L.J., Howard, R.M., Mulholland, K.R., Flitsch, S.L., Turner, N.J., 2016. One-Pot cascade synthesis of mono- and disubstituted piperidines and pyrrolidines using carboxylic acid reductase (CAR), ω-transaminase (ω-TA), and imine reductase (IRED) biocatalysts. ACS Catal. 6, 3753–3759. https://doi.org/10.1021/acscatal.6b00855.

Gallage, N.J., Hansen, E.H., Kannangara, R., Olsen, C.E., Motawia, M.S., Jørgensen, K., Holme, I., Hebelstrup, K., Grisoni, M., Møller, B.L., 2014. Vanillin formation from ferulic acid in *Vanilla planifolia* is catalysed by a single enzyme. Nat. Commun. 5, 4037. https://doi.org/10.1038/ncomms5037.

Gopal, M.R., Dickey, R.M., Butler, N.D., Talley, M.R., Nakamura, D.T., Mohapatra, A., Watson, M.P., Chen, W., Kunjapur, A.M., 2023. Reductive enzyme cascades for valorization of polyethylene terephthalate deconstruction products. ACS Catal. 4778–4789. https://doi.org/10.1021/acscatal.2c06219.

Gruez, A., Roig-Zamboni, V., Grisel, S., Salomoni, A., Valencia, C., Campanacci, V., Tegoni, M., Cambillau, C., 2004. Crystal structure and kinetics identify *Escherichia coli* YdcW gene product as a medium-chain aldehyde dehydrogenase. J. Mol. Biol. 343, 29–41. https://doi.org/10.1016/j.jmb.2004.08.030.

Hanefeld, U., Hollmann, F., Paul, C.E., 2022. Biocatalysis making waves in organic chemistry. Chem. Soc. Rev. 51, 594–627. https://doi.org/10.1039/D1CS00100K.

Hansen, E.H., Møller, B.L., Kock, G.R., Bünner, C.M., Kristensen, C., Jensen, O.R., Okkels, F.T., Olsen, C.E., Motawia, M.S., Hansen, J., 2009. De Novo biosynthesis of vanillin in fission yeast (*Schizosaccharomyces pombe*) and Baker's yeast (*Saccharomyces cerevisiae*). Appl. Environ. Microbiol. 75, 2765–2774. https://doi.org/10.1128/AEM.02681-08.

Hepworth, L.J., France, S.P., Hussain, S., Both, P., Turner, N.J., Flitsch, S.L., 2017. Enzyme cascades in whole cells for the synthesis of chiral cyclic amines. ACS Catal. 7, 2920–2925. https://doi.org/10.1021/acscatal.7b00513.

Ho, K.K., Weiner, H., 2005. Isolation and characterization of an aldehyde dehydrogenase encoded by the *aldB* gene of *Escherichia coli*. J. Bacteriol. 187, 1067–1073. https://doi.org/10.1128/JB.187.3.1067-1073.2005.

Horvat, M., Fritsche, S., Kourist, R., Winkler, M., 2019. Characterization of type IV carboxylate reductases (CARs) for whole cell-mediated preparation of 3-hydroxytyrosol. ChemCatChem 11, 4171–4181. https://doi.org/10.1002/CCTC.201900333.

Horvat, M., Weilch, V., Rädisch, R., Hecko, S., Schiefer, A., Rudroff, F., Wilding, B., Klempier, N., Pátek, M., Martínková, L., Winkler, M., 2022. Chemoenzymatic one-pot reaction from carboxylic acid to nitrile via oxime. Catal. Sci. Technol. 12, 62–66. https://doi.org/10.1039/D1CY01694F.

Horvat, M., Winkler, M., 2020. In vivo reduction of medium- to long-chain fatty acids by carboxylic acid reductase (CAR) enzymes: limitations and solutions. ChemCatChem 12, 5076–5090. https://doi.org/10.1002/cctc.202000895.

Jaeger, M., Rothacker, B., Ilg, T., 2008. Saturation transfer difference NMR studies on substrates and inhibitors of succinic semialdehyde dehydrogenases. Biochem. Biophys. Res. Commun. 372, 400–406. https://doi.org/10.1016/j.bbrc.2008.04.183.

Jo, J.-E., Mohan Raj, S., Rathnasingh, C., Selvakumar, E., Jung, W.-C., Park, S., 2008. Cloning, expression, and characterization of an aldehyde dehydrogenase from *Escherichia coli* K-12 that utilizes 3-Hydroxypropionaldehyde as a substrate. Appl. Microbiol. Biotechnol. 81, 51–60. https://doi.org/10.1007/s00253-008-1608-x.

Kallio, P., Pásztor, A., Thiel, K., Akhtar, M.K., Jones, P.R., 2014. An engineered pathway for the biosynthesis of renewable propane. Nat. Commun. 5, 4731. https://doi.org/10.1038/ncomms5731.

Knorr, S., Sinn, M., Galetskiy, D., Williams, R.M., Wang, C., Müller, N., Mayans, O., Schleheck, D., Hartig, J.S., 2018. Widespread bacterial lysine degradation proceeding via glutarate and L-2-hydroxyglutarate. Nat. Commun. 9, 5071. https://doi.org/10.1038/s41467-018-07563-6.

Kumar, P., Meza, A., Ellis, J.M., Carlson, G.A., Bingman, C.A., Buller, A.R., 2021. scp>l</scp> -threonine transaldolase activity is enabled by a persistent catalytic intermediate. ACS Chem. Biol. 16, 86–95. https://doi.org/10.1021/acschembio.0c00753.

Kunjapur, A.M., Cervantes, B., Prather, K.L.J., 2016. Coupling carboxylic acid reductase to inorganic pyrophosphatase enhances cell-free in vitro aldehyde biosynthesis. Biochem. Eng. J. 109, 19–27. https://doi.org/10.1016/j.bej.2015.12.018.

Kunjapur, A.M., Prather, K.L.J., 2015. Microbial engineering for aldehyde synthesis. Appl. Environ. Microbiol. 81 https://doi.org/10.1128/AEM.03319-14.

Kunjapur, A.M., Tarasova, Y., Prather, K.L.J., 2014. Synthesis and accumulation of aromatic aldehydes in an engineered strain of *Escherichia coli*. J. Am. Chem. Soc. 136, 11644–11654. https://doi.org/10.1021/ja506664a.

Lin, B., Tao, Y., 2017. Whole-cell biocatalysts by design. Microb. Cell Factories 16, 106. https://doi.org/10.1186/s12934-017-0724-7.

Neumann, M., Mittelstädt, G., Iobbi-Nivol, C., Saggu, M., Lendzian, F., Hildebrandt, P., Leimkühler, S., 2009. A periplasmic aldehyde oxidoreductase represents the first molybdopterin cytosine dinucleotide cofactor containing molybdo-flavoenzyme from *Escherichia coli*. FEBS J. 276, 2762–2774. https://doi.org/10.1111/j.1742-4658.2009.07000.x.

Orbegozo, T., Lavandera, I., Fabian, W.M.F., Mautner, B., de Vries, J.G., Kroutil, W., 2009. Biocatalytic oxidation of benzyl alcohol to benzaldehyde via hydrogen transfer. Tetrahedron 65, 6805–6809. https://doi.org/10.1016/j.tet.2009.06.088.

Pyne, M.E., Kevvai, K., Grewal, P.S., Narcross, L., Choi, B., Bourgeois, L., Dueber, J.E., Martin, V.J.J., 2020. A yeast platform for high-level synthesis of tetrahydroisoquinoline alkaloids. Nat. Commun. 11, 3337. https://doi.org/10.1038/s41467-020-17172-x.

Rodriguez, G.M., Atsumi, S., 2014. Toward aldehyde and alkane production by removing aldehyde reductase activity in *Escherichia coli*. Metab. Eng. 25, 227–237. https://doi.org/10.1016/j.ymben.2014.07.012.

Rodríguez-Zavala, J.S., Allali-Hassani, A., Weiner, H., 2006. Characterization of *E. coli* tetrameric aldehyde dehydrogenases with atypical properties compared to other aldehyde dehydrogenases. Protein Sci. 15, 1387–1396. https://doi.org/10.1110/ps.052039606.

Sadler, J.C., Wallace, S., 2021. Microbial synthesis of vanillin from waste poly(ethylene terephthalate). Green Chem. 23, 4665–4672. https://doi.org/10.1039/D1GC00931A.

Schaffer, J.E., Reck, M.R., Prasad, N.K., Wencewicz, T.A., 2017. β-Lactone formation during product release from a nonribosomal peptide synthetase. Nat. Chem. Biol. 13, 737–744. https://doi.org/10.1038/nchembio.2374.

Schwendenwein, D., Fiume, G., Weber, H., Rudroff, F., Winkler, M., 2016. Selective enzymatic transformation to aldehydes *in vivo* by fungal carboxylate reductase from *Neurospora crassa*. Adv. Synth. Catal. 358, 3414–3421. https://doi.org/10.1002/adsc.201600914.

Scott, T.A., Heine, D., Qin, Z., Wilkinson, B., 2017. An L-threonine transaldolase is required for L-threo-β-hydroxy-α-amino acid assembly during obafluorin biosynthesis. Nat. Commun. 8, 15935 https://doi.org/10.1038/ncomms15935.

Sheppard, M.J., Kunjapur, A.M., Prather, K.L.J., 2016. Modular and selective biosynthesis of gasoline-range alkanes. Metab. Eng. 33, 28–40. https://doi.org/10.1016/j.ymben.2015.10.010.

Sheppard, M.J., Kunjapur, A.M., Wenck, S.J., Prather, K.L.J., 2014. Retro-biosynthetic screening of a modular pathway design achieves selective route for microbial synthesis of 4-methyl-pentanol. Nat. Commun. 5, 5031. https://doi.org/10.1038/ncomms6031.

Slabu, I., Galman, J.L., Lloyd, R.C., Turner, N.J., 2017. Discovery, engineering, and synthetic application of transaminase biocatalysts. ACS Catal. 7, 8263–8284. https://doi.org/10.1021/acscatal.7b02686.

Son, J., Choi, I.H., Lim, C.G., Jang, J.H., Bang, H.B., Cha, J.W., Jeon, E.J., Sohn, M.G., Yun, H.J., Kim, S.C., Jeong, K.J., 2022. Production of cinnamaldehyde through whole-cell bioconversion from *trans* -cinnamic acid using engineered *Corynebacterium glutamicum*. J. Agric. Food Chem. 70, 2656–2663. https://doi.org/10.1021/acs.jafc.1c07398.

Song, W., Wang, J.-H., Wu, J., Liu, J., Chen, X.-L., Liu, L.-M., 2018. Asymmetric assembly of high-value α-functionalized organic acids using a biocatalytic chiral-group-resetting process. Nat. Commun. 9, 3818. https://doi.org/10.1038/s41467-018-06241-x.

Sulzbach, M., Kunjapur, A.M., 2020. The pathway less traveled: engineering biosynthesis of nonstandard functional groups. Trends Biotechnol. 38, 532–545. https://doi.org/10.1016/j.tibtech.2019.12.014.

Wannier, T.M., Nyerges, A., Kuchwara, H.M., Czikkely, M., Balogh, D., Filsinger, G.T., Borders, N.C., Gregg, C.J., Lajoie, M.J., Rios, X., Pál, C., Church, G.M., 2020. Improved bacterial recombineering by parallelized protein discovery. Proc. Natl. Acad. Sci. U. S. A. 117, 13689–13698. https://doi.org/10.1073/pnas.2001588117.

Winkler, M., Horvat, M., Schiefer, A., Weilch, V., Rudroff, F., Pátek, M., Martínková, L., 2022. Organic acid to nitrile: a chemoenzymatic three-step route. Adv. Synth. Catal. https://doi.org/10.1002/adsc.202201053 n/a.

Xu, L., Wang, L.-C., Su, B.-M., Xu, X.-Q., Lin, J., 2020. Multi-enzyme cascade for improving β-hydroxy-α-amino acids production by engineering L-threonine transaldolase and combining acetaldehyde elimination system. Bioresour. Technol. 310, 123439 https://doi.org/10.1016/j.biortech.2020.123439.

Xu, L., Wang, L.-C., Xu, X.-Q., Lin, J., 2019. Characteristics of <scp>l</scp> -threonine transaldolase for asymmetric synthesis of β-hydroxy-α-amino acids. Catal. Sci. Technol. 9, 5943–5952. https://doi.org/10.1039/C9CY01608B.